UNIVERSITY OF LEEDS

Department of Physics and Astronomy

BSc Project

PHYS3150

Herbig Ae/Be Star Accretion Rates and the Hertzsprung Russell Diagram

Author:
Alison McSloy
Student number:
200549097

Supervisor:
Professor Rene Oudmaijer

Submission date: 11th February 2013

Word count: 3850

1 Abstract

The accretion rates of a sample of 90 Herbig Ae/Be stars were calculated, using photometry data from the X shooter project at the European Southern Observatory's Very Large Telescope. Accretion rate estimates for Herbig stars have been studied far less than those for low mass stars, demonstrating the importance of conducting further research in this area. The strength of the observed hydrogen α lines for each star were used to calculate the accretion rate values. The data for the Herbig stars was plotted on a Hertzsprung-Russell diagram. The accretion rates calculated varied from 10^{-5} - 10^{-11} $M_{\odot}yr^{-1}$. The median mass accretion rate was found to be 5 x 10^{-8} $M\odot yr^{-1}$. A positive correlation was found between stars' accretion rates and their bolometric luminosities, as well as between stars' accretion rates and their temperatures.

2 Introduction

The formation of stars from the interstellar medium is a physical process that is still not fully understood by astronomers today. There are many parameters that affect the rate of star formation that must be considered, such as angular momentum, metallicity, stellar and circumstellar masses, the environment in which the star formation occurs, and time [1]. In recent years, low mass star formation, namely the formation of T Tauri stars, has been well studied; as a result the physical processes involved in creating these stars are now fairly well understood. High mass star formation is slightly less well understood, but the real gap in knowledge arises at the interface between the two. The physical processes present in formation of intermediate mass stars, i.e. Herbig stars, remains largely unknown. It is this lack of current knowledge that emphasises the importance of continuing research into this topic, in order to allow astronomers to construct theories that could explain how these intermediate mass stars are formed.

Low mass star formation (typically <2M⊙) is accepted to occur by a process called magnetospheric accretion [2]. In contrast, high mass star formation is not understood quite as well, similar accretion rates would result in high mass stars leaving the Zero Age Main Sequence before becoming fully formed. As this is not observed, another form of accretion must occur in order for high mass stars to form [3]. The point where the magnetospheric accretion process stops and another accretion process begins is currently unknown, but it is clear that studying these intermediate mass (2-10M⊙) stars will allow astronomers to further their understanding in this area. The point where magnetospheric accretion stops and another accretion mechanism begins is currently unknown; this topic is still debated today. There have been very few direct observations of Herbig star magnetic fields to date [4], meaning that the origin of these magnetic fields still remains a mystery [5]. This further supports the view that more research must be carried out in order to improve astronomers' understanding of this intermediate mass star formation. This project investigates the accretion rates of Herbig Ae/Be stars, which are an example of these intermediate mass stars.

Herbig Ae/Be stars are intermediate mass stars (2-10M⊙) that are still in the pre-Main Sequence contraction phase [6]. Herbig stars are defined as stars with spectral type A or B (with emission lines), that exhibit an infrared excess, and are within luminosity classes III-V. This definition will unavoidably include some evolved massive stars, so it is imperative that astronomers must take care to differentiate between these and Herbig stars [8].

It is worth taking a moment to define accretion rates themselves. Stars form within giant molecular clouds (hereafter referred to as GMCs), which have masses in the range of 10^3M⊙-^{7}M⊙ [9]. The average density of these GMCs is 10^2-10^3 particles per cm^3 [10]. A large proportion of the matter found between these forming stars is gas, where hydrogen exists in atomic form [11]. When a protostar of mass M and radius R accretes some mass δm during the formation process, its gravitational potential energy decreases. This accretion of mass occurs over a time δt, which allows the average rate of gravitational energy release to be calculated. This average value is proportional to the average mass accretion rate by the following equation:

$$E_{grav} = \frac{GM\dot{M}}{R} \quad (1)$$

In order to remain in thermal equilibrium, the rate of gravitational energy released must equal the accretion luminosity; if this energy is not efficiently radiated away, the protostar's temperature would increase. If this assumption is followed, an accretion luminosity can be defined [12]:

$$L_{acc} = \frac{GMM_{acc}}{R_*} \tag{2}$$

In the case of Herbig stars, material accretes onto the star via an accretion disc, which in some cases can be directly observed. For example, the dust component of the disc can be observed via the scattering of optical and near-infrared light [11]. The geometry of Herbig star accretion discs is still under investigation; however, it is widely accepted that as dust grains coagulate, they settle towards the midplane of the disc, making them easier to observe [13]. However, this only applies to Herbig stars close enough to the observer; the majority of the time, these accretion discs cannot be directly observed. As accretion discs are often not directly observable, other methods must be used in order to provide proof their existence. An example of such a method is the measurement of disc velocity profiles, which imply the presence of a rotating disc around a star. These profiles reveal velocity gradients, which indicate the presence of material orbiting a protostar in a disc-like configuration [14].

Emission lines can be used to calculate mass accretion rates for stars. From the above explanation of accretion rates, it is not immediately obvious how one can calculate an accretion rate given an emission spectrum. In order to understand how measuring emission lines can result in a calculated accretion rate, one must consider the physical processes that occur when a protostar accretes mass from its surrounding disc. As described by equation 2, when matter accretes onto a protostar, the resulting loss in gravitational potential energy is released as luminosity. When material accretes onto a protostar, all of this material is heated to approximately the same temperature, resulting in the observation of blackbody radiation (due to the accreting material). The protostar itself also produces a certain luminosity, so it follows that the observed spectra is a combination of the two different luminosities. When the spectra are observed, these luminosities are measured as fluxes; the relation between these two parameters is shown in equation 3. An example of the difference between a star's luminosity and the accretion luminosity is illustrated in figure 1, for a protostar of M_*=2.5$M_\odot$ and R_*=2.6$R_\odot$:

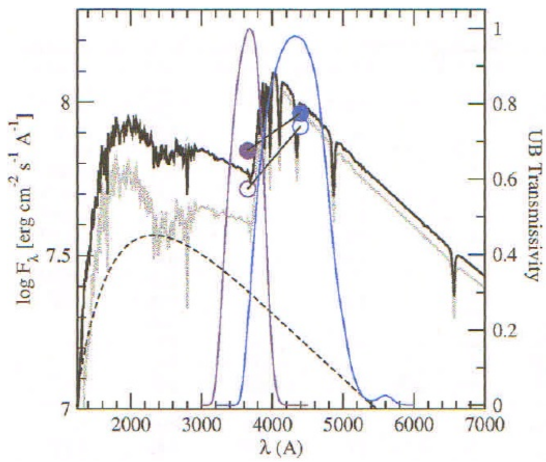

Figure 1: Example of total flux due to accretion and a protostar [15]

In Figure 1, the black line represents the observed spectra of a star. The grey line represents the contribution to the total flux from the star itself, and the dashed line illustrates the contribution to the total flux from the accretion luminosity.

Some of this blackbody radiation (due to the accreting material) acts to ionise the hydrogen atoms in the surrounding disc. When the hydrogen then recombines, emission is produced, accounting for the emission lines present in the observed spectra. The strength of the hydrogen α emission line has been shown to increase with the accretion luminosity of a star [15]. For this reason, the hydrogen α line acts as an excellent tracer of accretion rates.

Now that the reason for using the hydrogen α emission line as a tracer of accretion rates has been determined, the process of calculating an accretion rate can be explained. The first step in this process is to measure the equivalent width of an emission line, for example the hydrogen α emission line at 6562.6Å. This equivalent width is a way of measuring the relative strength of the emission line. The flux of the hydrogen α line can then be calculated by multiplying the equivalent width by the flux density of the R band. From this, the line luminosity can be calculated from the following equation:

$$L = 4\pi d^2 f \tag{3}$$

where f is the line flux, d is the distance to the star, and L is the line luminosity. The line luminosity can then be converted into an accretion luminosity, which in turn leads to the calculation of an accretion rate. Parameters such as distance d, mass M and radius R are usually found in photometry data, or can be sourced from other papers.

3 Data and Flux Measurements

The photometry data and spectra of the 90 Herbig Ae/Be stars that were analysed were taken from the X shooter project, which is a medium resolution spectrometer mounted on the European Southern Observatory's Very Large Telescope. The X shooter project is revolutionary in the field of astrophysics, and has proven to be an invaluable resource in the study of many different astronomical objects. The norm for data collection is to conduct several exposures at different wavelength bands, which can take up to several hours of precious telescope time. The X-shooter is different; it can take the entire spectra of an object in one exposure time, which is a far more efficient use of both time and resources. The wavelength band the X-shooter project can collect data for is 3000-25000$\mathring{A}$.

The Spectral Analysis Tool (SPLAT) was used to measure equivalent width values for the hydrogen α lines. To obtain this value, the background continuum level of a spectrum was defined, and a polynomial was fitted to the emission peak (in this case the hydrogen α line at 6562.8$\mathring{A}$). Using the equivalent width is an excellent method for calculating accretion rates, as the same result for each spectra will be obtained regardless of the resolution. The area under the emission peak is then compared to the background continuum; the width of the areas with respect to the continuum is the equivalent width.

One point for consideration at this stage of the calculation was the effect of intrinsic absorption. This process was ignored when calculating equivalent widths, but could have had an effect on the resulting accretion rate value. For approximately 40 stars, there was some intrinsic absorption present in the spectra, resulting in a visible "dip" from the background continuum present on both sides of the hydrogen α emission peak. The consideration of intrinsic absorption would have resulted in higher equivalent width values for these stars. Underlying absorption present in an emission line may not be at all observable, so it could be the case that all 90 stars analysed were affected by this This higher equivalent width value would then result in a higher value of the accretion rate.

Once the equivalent width has been found, the flux density must also be calculated in order to achieve a value for the line flux. The photometry data consisted of two tables provided by the supervisor. They contained data acquired from various sources, which was then compiled into the photometry data used. Apparent magnitudes at each band in the UBVRI photometric system and the extinction values (at the V band) were given. The extinction at the R band was calculated by a simple conversion:

$$A_R = 0.748 A_V \tag{4}$$

where A_V is the extinction at the V band, and A_R is the extinction at the R band. The apparent magnitude at the R band was then "de-reddened" by subtracting the extinction at the R band, and the resulting magnitudes were then converted to flux densities. The R band wavelength peaks at 6580$\mathring{A}$, which includes the hydrogen α wavelength, hence why this was the only wavelength band considered for this data set. The line flux "f" could then be calculated by multiplying the flux density by the equivalent width. The line flux values were then used to calculate the line luminosities using equation 3.

4 Analysis

After the flux measurements were obtained, the accretion luminosity could be calculated. The equation used to convert from line luminosity to accretion luminosity is as follows [15]:

$$log\frac{L_{acc}}{L\odot} = 2.28(\pm0.25) + 1.09(\pm0.16) \times log\frac{L_{H\alpha}}{L\odot} \tag{5}$$

where L_{acc} is the accretion luminosity, and $L_{H\alpha}$ is the hydrogen α line luminosity. In order to calculate the final value for the accretion rate, masses and radii of all 90 stars needed to be calculated. The spectral type for each star was listed in the photometry data; this was used to find the typical mass and radius for each spectral type, using values obtained from a paper [16]. As no pre-Main Sequence values were available, values from the Zero Age Main Sequence (hereafter referred to as ZAMS) and class

V data were used. As all necessary parameters had now been calculated, the final accretion rate could then be calculated for each star using the following equation:

$$M_{acc} = \frac{L_{acc} R_*}{G M_*} \tag{6}$$

where M_{acc} is the accretion rate, L_{acc} is the accretion luminosity, R_* is the radius of the star, G is the universal gravitational constant $G=6.67 \times 10^{-11}$, and M_* is the mass of the star.

Sixteen stars in the photometry data had no listed distance and/or bolometric luminosity; as these parameters are essential for the calculation of accretion rates and plotting points on the HR diagram, these stars were excluded from the final results. Therefore, the HR diagram shown in Figure 1 contains only the 74 stars that accretion rates were calculated for.

As there are several separate steps involved in calculating the accretion rates, it is obvious that there would be several errors to consider when estimating the final error in the result. Errors could be estimated for the equivalent width, the R band magnitude, the extinction, and the distance. The main contribution to the error in the accretion rate values was due to the distance values used, which will be discussed in further detail in section 6.

Further analysis was conducted in order to determine the correlation (if any) between accretion rate and temperature/bolometric luminosity. This process involved splitting the data points into 3 evolutionary groups, by assuming the evolutionary tracks themselves were approximately horizontal. This was a reasonable assumption to use, as previous calculations of evolutionary tracks have been shown to tend towards a horizontal (as opposed to vertical) orientation. An example of such evolutionary tracks are shown in Figure 2 below:

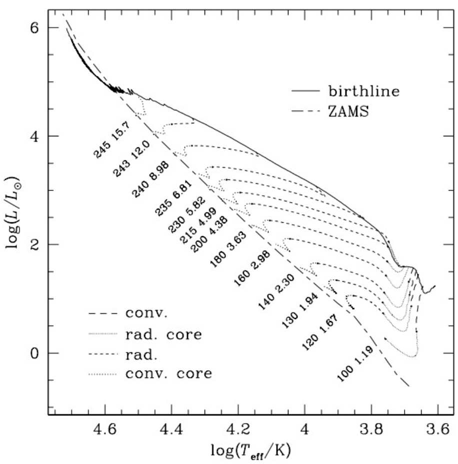

Figure 2: Evolutionary tracks leading to the ZAMS. Coupled numbers show the age of the star (in 10^3 yr) after accretion has ceased, and the mass (in M$\odot$) at that time, when the star has arrived on the ZAMS. [3]

5 Results

Figure 1 shows the HR diagram containing the 74 stars with their calculated accretion rates, as well as an overlay of the Zero Age Main Sequence. The strength of each accretion rate is represented via the size of the data point on the graph; the larger the data point, the higher the accretion rate. For clarification, a data point in the subset 5 has an accretion rate of 10^{-5} M$\odot$yr^{-1}, and a data point in the subset 11 has an accretion rate of 10^{-11} M$\odot$yr^{-1}.

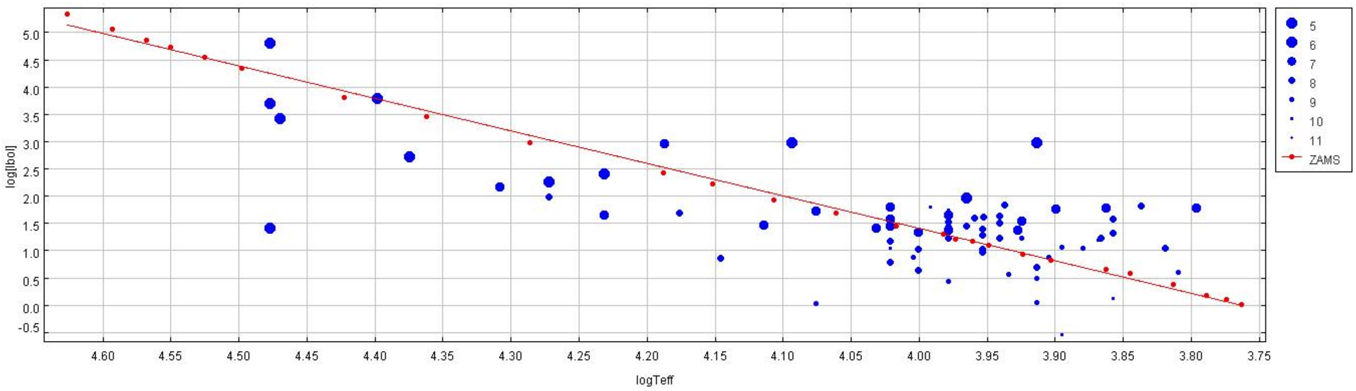

Figure 3: Herbig stars with the Zero Age Main Sequence overlaid

The evolutionary tracks of Herbig stars within the HR diagram were assumed to be horizontal, to allow for further data analysis. The data points were split into 3 different evolutionary groups depending on their bolometric luminosities. A positive correlation was found for a plot of accretion rate vs. bolometric luminosity; the results are shown in figure 4 below.

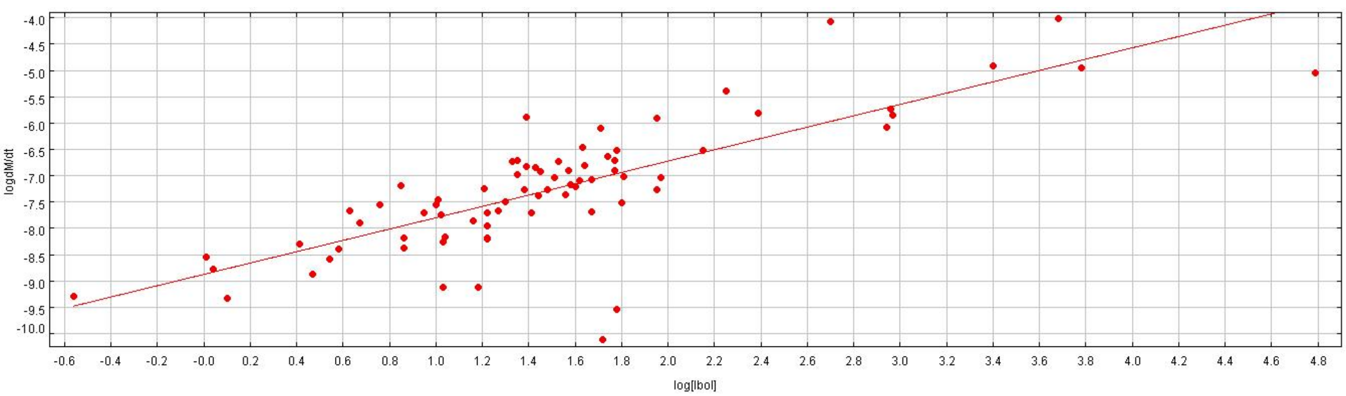

Figure 4: Plot of accretion rate vs. bolometric luminosity

The same graphs were plotted for all 3 defined evolutionary tracks, so that individual trends (if any) could be identified. As all groups gave similar correlations, only the lower of these evolutionary tracks is shown below in Figure 5, for simplicity.

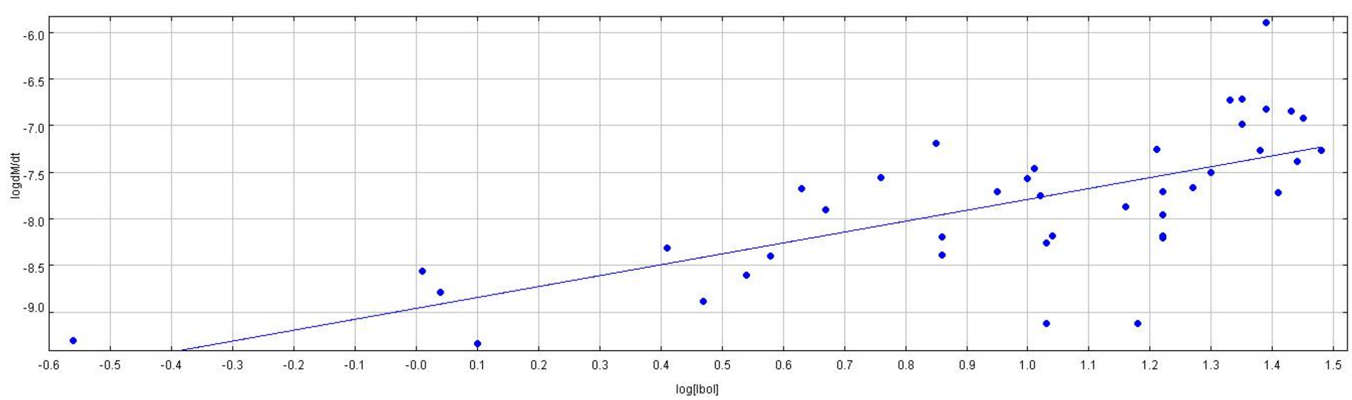

Figure 5: Accretion rate vs. bolometric luminosity for lowest evolutionary track

A positive correlation was also found for accretion rate and temperature, as shown in Figure 6:

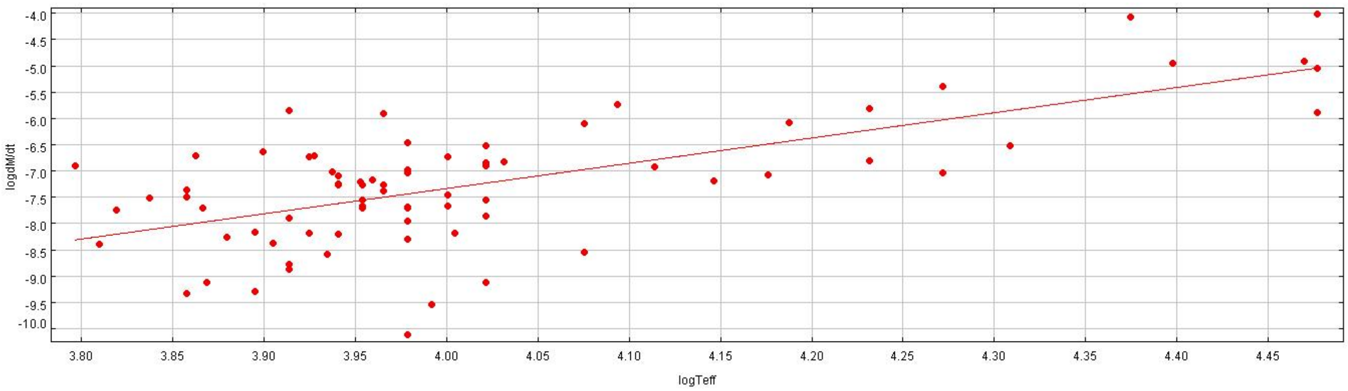

Figure 6: Plot of accretion rate vs. temperature

As with the correlation between accretion rate and bolometric luminosity, similar trends were found for all 3 evolutionary groups. Therefore, the results for the lower evolutionary group (in terms of bolometric luminosity) only is shown in Figure 7:

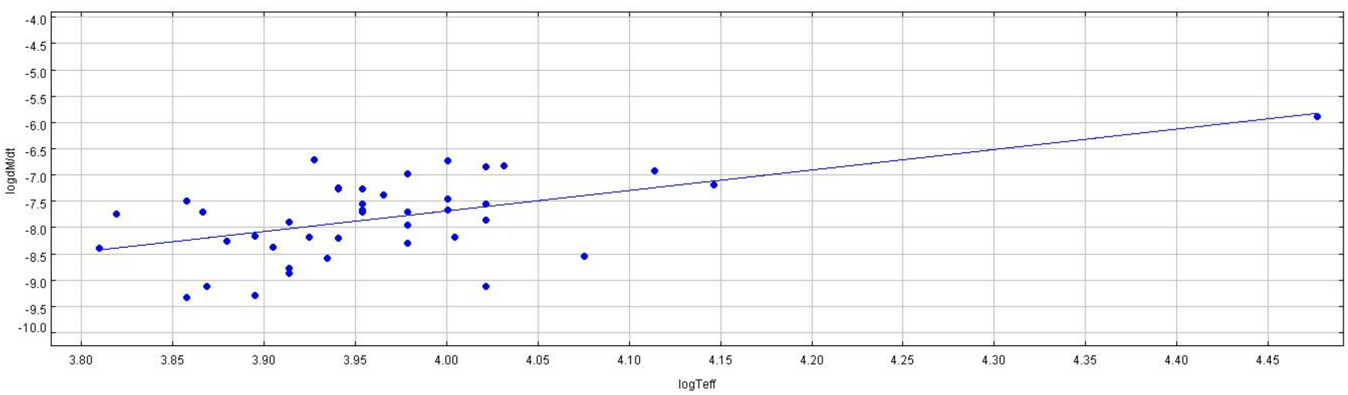

Figure 7: Plot of accretion rate vs. temperature

6 Discussion

The above results lead to many interesting points of discussion. The overlay of the Zero Age Main Sequence (hereafter referred to as the ZAMS) on the data points for the Herbig stars does not appear where one might expect. Previous papers [6] have predicted evolutionary tracks that imply Herbig stars should be located above and to the right of the Main Sequence (hereafter referred to as the MS). Figure 3 illustrates this is not the case for this set of data. However, there are some points that could account for this discrepancy. Firstly, the MS is not a distinct line, as plotted in figure 3; the MS does have a particular width. This width can be estimated by the difference between the MS and the ZAMS.

The values of bolometric luminosity included in the photometry data also offer an explanation of the position of the ZAMS line in Figure 3. When compared to existing research papers, some discrepancies between the values are evident. One example is HD150193 - in the photometry data, the value of $\log L_{bol}$ is given as 1.01. In a previously published paper, the value for the same star is given as $\log L_{bol}=1.47$ [6].Using the value given by the photometry data, this particular star is found to lie below the ZAMS, whereas the alternative value for the bolometric luminosity would move it to above the ZAMS. If the general trend of underestimating the bolometric luminosities was found, all points could lie above the ZAMS line. This would then support the theory that Herbig stars evolve from right to left across the HR diagram onto the MS, which is illustrated in figure 2.

Finally, another possible reason for the layout of the results in figure 3 is the errors in the luminosity.

Distance to the star is the least accurate measurement, subject to up to 50% error. As luminosities values are proportional to the value of the distance squared, it is reasonable to assume that the error in the logL_{bol} values could be up to 30%. If we assume the values have all been underestimated by this amount, all data points would lie above the ZAMS, as expected.

Another point to consider is the effect of intrinsic absorption, which was previously discussed in the "Data and Flux Measurements" section. Not accounting for intrinsic absorption effects results in a lower accretion rate value. For stars with spectra that showed intrinsic absorption, correcting for this effect would result in higher calculated accretion rates. Although a different accretion rate would not affect where the star would lie on the HR diagram, it could potentially affect the trend in the data.

The trend in the data for the HR diagram (shown in Figure 3) appears to be that stars with higher temperatures have higher accretion rates. This trend supports the theory - the hotter a protostar is (i.e. the higher its luminosity), the more massive it tends to be. A Mass-Luminosity relation does exist, but is only applicable to Main Sequence stars. For Pre-Main Sequence, a relation between luminosity, radius and temperature has been derived [7]:

$$L = R^2 T^4 \quad (7)$$

where L is the luminosity (in terms of solar luminosities), R is the radius of the star, and T is the temperature of the star. If a protostar is more massive, it follows that it should accrete more material than that of a low mass protostar. Therefore it follows that protostars with stronger accretion rates should also have higher temperatures, which is observed in the data.

Figures 4 and 5 show the correlation between accretion rate (log$\frac{dM}{dt}$) and bolometric luminosity (logL_{bol}) - figure 4 shows the correlation for all data points, and figure 5 shows the correlation for the lower bolometric luminosity evolutionary group. It is clear to see a positive correlation exists between the accretion rate and the bolometric luminosity. The same result is found for the correlation between accretion rate and temperature. The bolometric luminosity correlation is perhaps slightly stronger than that for temperature; this can be explained by considering the relationship between luminosity and temperature, shown in equation 8:

$$L = 4\pi R^2 \sigma T^4 \quad (8)$$

where L is the bolometric luminosity, R is the radius of the star, σ is the Stefan Boltzmann constant (5.67 x 10^{-8} $Wm^{-2}K^{-4}$), and T is the surface temperature of the star. It can be seen that luminosity is proportional to the square of the radius and the temperature to the 4th power. As luminosity increases, the temperature increases by a far larger factor, leading to a slightly weaker correlation.

7 Conclusion

These results represent the largest data set of Herbig Ae/Be star accretion rates ever analysed. The median mass accretion rate was found to be 5 x 10^{-8} $M_\odot yr^{-1}$, with accretion rates ranging from 10^{-5} $M_\odot yr^{-1}$ to 10^{-11} $M_\odot yr^{-1}$. Errors in calculations were discussed for all relevant variables in section 6. The dominant contribution to the error in the accretion rate calculations was found to be the distance, where values could have up to 50% error.

The hydrogen α lines were used as accretion tracers successfully, to observe if a trend existed for these accretion rates when plotted on a Hertzsprung Russell diagram. Intrinsic absorption was not taken into account when measuring equivalent widths; however, the consequences of this have been discussed throughout. There appears to be a correlation between the accretion rate of a star and its temperature/bolometric luminosity; as a star's temperature and/or the bolometric luminosity increases, so does its accretion rate. From section 6, it is clear to see that this trend supports the theory.

Although the ZAMS overlay is not where one would expect, several reasons to account for this have been discussed. For example, the bolometric luminosity values could have been underestimated in the photometry data; if this had been corrected, all data points may have been positioned to the right of the ZAMS line. This analysis presents the possibility of a point for future work, which is discussed in section 8.

Positive correlation between both accretion rate vs. bolometric luminosity and accretion rate vs. temperature were also observed. As previously mentioned, the correlation with bolometric luminosity appears to be slightly stronger than the correlation with temperature. Reasons for this were discussed in section 6, and again future work that could be conducted to further analyse this trend is suggested in section 8.

8 Future Work

A possible avenue of research could be to re-examine the Hertzsprung Russell diagram. If all luminosities were positioned above the ZAMS line, one could calclate the distance of these stars from the ZAMS. The expectation could be that the further a star is from the ZAMS line, the higher its accretion rate would be. However, this is not necessarily the case, as these distances to the ZAMS have not yet been calculated.

Another point for future work could be to analyse the statistics of the correlations for both accretion rate vs. bolometric luminosity and accretion rate vs. temperature. Due to time constraints, these statistics were not calculated. By obtaining these statistics, the true correlations would be found, and it would be far easier to compare the two relationships between accretion rates and bolometric luminosity, and temperature.

9 References

[1] L. Waters & C. Waelkens. (1998) Herbig Ae/Be Stars. **Annual Review of Astronomy and Astrophysics**, 36(1), pp.233-66

[2] J. Bouvier et al. (2007) **Protostars and Planets V** 1st ed. Tucson: University of Arizona Press.

[3] R. Behrend & A. Maeder. (2001) Formation of massive stars by growing accretion rate. **Astronomy & Astrophysics** 373(1), pp.190-198

[4] S. Hubrig et al. (2004) Magnetic fields in Herbig Ae stars **Astronomy & Astrophysics** 428(1), pp.L1-L4.

[5] G.A. Wade et al. (2008) A search for strong, ordered magnetic fields in Herbig Ae/Be stars. **Monthly Notices of the Royal Astronomical Society**, 376(3), pp.1145-1161

[6] Van den Ancker et al. (1997) Hipparcos data on Herbig Ae/Be stars: an evolutionary scenario. **Astronomy & Astrophysics**, 324, L33-L36.

[7] S. Huang. (1961) Distribution of Pre-Main Stars in the H-R Diagram. **Astrophysical Journal**, 134, pp.12-19.

[8] Van den Ancker et al. (1998) Hipparcos photometry of Herbig Ae/Be stars. **Astronomy & Astrophysics**, 330, pp.145-154.

[9] N. Murray. (2011) Star formation efficiencies and lifetimes of Giant Molecular Clouds in the Milky Way. **The Astrophysical Journal**, 729(2), pp.133-147

[10] J. Williams et al. (2000) **Protostars and Planets V** 1st ed. Tucson: University of Arizona Press.

[11] S. Stahler & F. Palla. (2005) **Formation of Stars** 1st ed. Weinheim: Wiley-VCH.

[12] D. Prialnik. **An Introduction to the Theory of Stellar Structure and Evolution** 2nd ed. Cambridge: Cambridge University Press.

[13] G. Meeus et al. (2012) GASPS observations of Herbig Ae/Be stars with PACS/Herschel. The atomic and molecular content of their protoplanetary discs. **Astronomy & Astrophysics**, 544, A78.

[14] V. Mannings and J.I. Sargent (1997) A high-resolution study of gas and dust around young intermediate-mass stars: evidence for circumstellar disks in Herbig Ae systems. **The Astrophysical Journal**, 490, pp.792-802

[15] Mendigutia et al. (2011) Accretion rates and accretion tracers of Herbig Ae/Be stars. **Astronomy & Astrophysics**, 535, A99.

[16] Straizys and Kuriliene. (1981) Fundamental Stellar Parameters Derived from the Evolutionary Tracks. **Astrophysics and Space Science**, 80, pp.353-368.